Energy flux measurements during magnetron sputter deposition processes

Anne-Lise Thomann, Amaël Caillard, Muhsin Raza, Mariem El Mokh, Pierre-Antoine Cormier, Stephanos Konstantinidis

Energy flux measurements during magnetron sputter deposition processes

A.-L. Thomann*[1], A. Caillard[1], M. Raza[2], M. El Mokh[1], P.A. Cormier[1], S. Konstantinidis[2]

[1] Groupe de Recherches sur l'Energétique des Milieux Ionisés (GREMI), UMR7344

Université d'Orléans – CNRS BP6744, F-45067 Orléans Cedex 2, France

[2] Chimie des Interactions Plasma-Surface (ChIPS), Université de Mons, Avenue Copernic 3,

7000 Mons, Belgium

* Corresponding author: anne-lise.thomann@univ-orleans.fr

Keywords: Magnetron sputtering, energy flux, thin film deposition, sputtering process, crystalline phase formation

Abstract

The influence of energetic species on thin film growth mechanism is a long-term issue in the field of low-pressure plasma-based magnetron sputtering technology. Several species may contribute to the energy flux such a plasma ions, electrons and neutrals, film-forming species, photons, etc. Several research groups have designed probes capable of quantifying energy fluxes in these particular working conditions and experimental strategies to get a better insight on the relationship between the plasma working parameters, the energy flux, the film growth mechanism and the coating properties. In this paper we aim at showing how the thermopile-based probe developed at GREMI laboratory can contribute to this field thanks to its time resolved capability (~ms) and sensitivity (~mW/cm^2). We show how such a probe can be used to identify and quantify energetic contributions such as gas conduction, chemical reactions on surfaces such as oxidation, but also radiations emitted from a (hot) sputter target during DC,

pulsed-DC and High-power Impulse Magnetron Sputtering (HiPIMS) processes. Both non-reactive and reactive sputtering discharges are studied. Ultimately, we present data on the relationship between the phase composition and the energy deposited during the synthesis of two technologically important thin film materials, namely Titania and Zirconia. Through the reported examples, the advantage and limitations of energy flux measurements and the interest to couple the obtained data to those derived from conventional plasma diagnostics are discussed. The relative importance of various energetic contributions is investigated in a purpose to identify the key parameters driving the film properties.

1. Introduction

Knowing the energy influx (e.g. deposited power) at surfaces (walls, sputtering target, substrates, etc) is a key issue for controlling low pressure plasma-based processes, in particular those dedicated to material and surface processing such as etching and thin film deposition [1]. Indeed, the modification of the energy flux may dramatically influence material properties since the surface atomistic processes such as diffusion, island growth and crystallization, or phase (trans)formation strongly depend on the energy available at the substrate surface [2,3].

During plasma/surface interaction, energy can be transferred via various elementary mechanisms involving electrons, neutrals, ions, and/or photons. The total input power (P_E) is therefore the surface integral over all possible energy fluxes (J_{in}, energy delivered per unit time and area) as highlighted by the equation 1 here after:

$$P_E = \int J_{in} \cdot dS = \int (J_i + J_e + J_n + J_{rad} + J_{film}) \cdot dS \quad \text{(Eq 1)}$$

J_i, J_e and J_n are the contributions of ions, electrons, and neutrals, respectively. J_{rad} regroups the energy flux densities originating from radiation emitted by hot surfaces and plasma excited species, and J_{film} is the heat released during the condensation of film forming species, adsorption, chemical reactions, and phase transitions.

The total deposited energy can be estimated by evaluating each energy contribution. This requires the knowledge of each elementary mechanisms of energy transfer and the relative role that each species play in the total energy deposition. This estimation is difficult to achieve even when complementary gas phase/plasma diagnostics and/or simulations are implemented. Beside the fact that the estimation of every energy contribution (which requires knowing the flux and energy distribution function of each interacting species) is a complex and time-consuming task, this calculation is usually based on assumptions because some energy transfer

coefficients are not known. A way to overcome these drawbacks is to measure the total energy transferred to the surface during the plasma process using dedicated probes [1, 4-7].

Estimating the energy deposited at the substrate during plasma (magnetron) sputter deposition is quite an old issue and was already discussed by Thornton and Westwood [8, 9].

Several diagnostics based on various sensors have been used in magnetron sputtering processes such as calorimetric probe [1], Gardon radiometer [7], thermopile [10] etc. They allow either the direct measurement of the instantaneous energy flux density or an a *posteriori* evaluation of the total amount of transferred power. Several articles reported values of the energy flux at the substrate position during magnetron sputter deposition. Typical values lye in the 1 – 300 mW/cm^2 range [11-17]. Thornton and Lamb [11] calculated the Normalized Energy Flux (NEF) by dividing the total energy flux density by the number of metal atoms deposited per time unit. It typically ranges between 10 to 100 eV per deposited atom for light and heavy sputtered elements, respectively. This parameter is a convenient "standardization" parameter allowing to compare experiments performed in different environments. Drüsedau et al even evidenced that an empirical law relating the NEF to the atomic mass of the target element and to the sputtering yield permitted to predict experimental data obtained for a large range of materials with an accuracy of 30%. The typical values they found lye between 5 and 140 eV. The NEF increases up to the keV per molecule as the discharge operates in a so-called reactive Ar/O_2 atmosphere to deposit thin films like alumina or chromia from their respective metal targets [5,10]. Drusedau measured a NEF equal to 15.7 keV per atom during the growth of aluminum nitride coatings [12].

The interest of investigating the energetic conditions at the substrate is to unravel the relationship between energy deposition and the film properties, such as microstructure or phase composition. In 1994, Löbl *et al.* studied the link between the energy flux and the phase composition of titanium dioxide films prepared by evaporation and ion – based methods [17].

Various film growth processes were compared only considering the typical energy of the depositing particles. These authors proposed a semi-quantitative description of the evolution of the phase composition of titania films as a function of the NEF. The latter is presented in Fig 1.

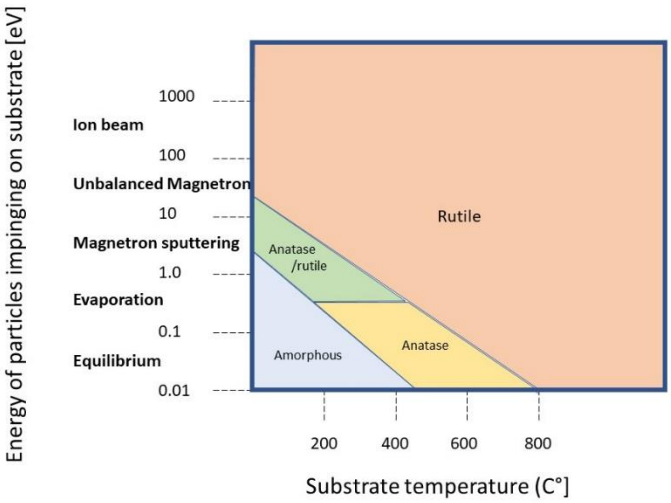

Fig. 1. Evolution of the phase composition of titanium dioxide thin films as a function of the typical impinging particle energy during growth, adapted from Löbl *et al*. [17].

From this figure, one can learn that amorphous films are obtained at low particle energy and substrate temperature. As the deposition temperature, i.e. the substrate surface temperature, is increased up to ~400°C, anatase crystallites form. At ~800°C, rutile crystals appear. An identical evolution was highlighted by N. Martin *et al.* as a function of the substrate temperature for amorphous TiO_2 films deposited on silicon and annealed afterward [18]. From the figure 1, it is seen that increasing the energy of the particle impinging on the substrate allows to produce anatase or even the high-temperature rutile phase, at lower substrate temperature. The higher the energy input from the incoming species, the lower the substrate temperature at which the rutile phase can be obtained. Mráz and Schneider further strengthened this statement by depositing TiO_2 films by magnetron sputtering in various working conditions [19]. When

plotting the phases formed depending on the ion energy flux, distinct boundaries for the deposition of anatase, rutile, and mixture of these two phases can be recognized, as reported in Fig 2.

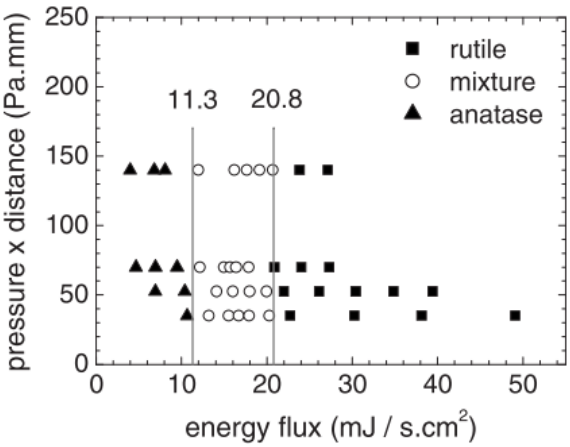

Fig. 2. "phase diagram" derived by Mráz and Schneider [19] when studying the evolution of the phase composition of TiO_2 films with respect to the (working) pressure x distance (between the sputter target and the substrate) and the ion energy flux.

The authors drew two distinct boundaries on the graph presented in Fig 2. When dividing the ion energy flux by the metal atom flux that is assumed to be constant in the investigated range of parameters (unchanged power supplied to the cathode), these boundaries appears at 540 eV/Ti atom and 1000 eV/Ti. Pure anatase thin films are grown below the lowest value while pure rutile thin films are obtained above the highest value. Between these two boundaries, an anatase/rutile phase mixture is obtained.

Mráz and Schneider suggested that the ratio between the ion energy flux and the deposition flux governs the phase formation of magnetron sputtered TiO_2 thin films. The other conclusion that can be drawn from the Fig. 2 is that the mean kinetic energy brought by the film forming particles determined by the *P x d* (pressure x target-to-substrate distance) product, does not play a dominant role in their work. Indeed, at a constant ion energy flux value, no phase transition

is observed on the graph as the *P x d* parameter varies. This could seem contradictory with results from Löbl *et al*. who clearly relate the phase composition to this parameter. One has to keep in mind that Löbl's work gives general trends depending on the deposition technique whereas Mráz and Schneider focused their study on a given magnetron sputtering experiment. The obtained values by Mráz and Schneider are higher than those evaluated by Löbl *et al* by roughly on order of magnitude (Fig. 1). This is because in Mraz's work the only contribution considered is that of the plasma (Ar^+ ions). These authors inferred the energy flux from energy resolved mass spectrometry and electrostatic probe measurements [19]. On the contrary, as mentioned above, estimations given by Löbl take into account the typical energy deposited by Ti atoms depending on the deposition technique. Thus, in both works, the global energy deposited at the substrate during the process is ignored. From these two studies, it can be concluded that, independently on the specie bringing the energy to the surface (condensing atoms or plasma ions), the formation of anatase (rutile) phase is promoted when the energy brought to the surface is low (high).

Stranak and coworkers [20] also studied the deposition of TiO_2 films. Their experimental setup consisted of a High-Power Impulse Magnetron Sputtering system enhanced by an Electron Cyclotron Wave Resonance (ECWR) plasma located between the sputter target and the substrate. The (101) preferred orientation of the rutile phase found in the TiO_2 films changes as the pressure distance product (*Pxd*) increases. The (101) textured rutile film changes first towards randomly oriented rutile crystallites and the formation of the anatase phase follows. The energy flux measured at the substrate position using a calorimetric probe varies from 205 mW/cm^2 for a target-to-substrate distance of 30 mm and pressure of 0.08 Pa. It decreases down to 44 mW/cm^2 for a distance of 110 mm and a pressure of 10 Pa. From the data reported in their publication, one can estimate the NEF which is then calculated from the deposition rate

expressed in nm/min (See table 1 below) and by assuming a mean density of 4.25 g/cm^3 (3.08 10^{22} TiO_2/cm²).

Table 1. TiO_2 film properties prepared by the ECWR–HiPIMS system, the crystallographic phases, the deposition rates and the total energy flux densities are taken from [20]. The NEF values are obtained by assuming a TiO_2 density of 4.25 g/cm^3.

		30 mm	50 mm	70 mm	110 mm
0.08 Pa	*nm/min*	*2.7*	*1.3*	*0.5*	*0.3*
	mW/cm^2	205	116	130	126
	keV/at$_{Ti}$	8.9	10.5	30.5	49.2
	Phase	R pref. O	R	R	R
10 Pa	*nm/min*	*0.9*	*0.3*	*0.2*	*0.1*
	mW/cm^2	126	76	51	44
	keV/at$_{Ti}$	16.4	29.5	29.9	51.6
	Phase	R	R	R+A	A

Obtained NEF values are quite high (up to 51.6 keV/at), and, at first glance, the reported trends appear in opposition with those previously presented since here anatase phase is formed at the highest NEF values. However, in their work the authors show that more than 80% of the total power flux comes from the ECWR plasma (mainly from electrons) and principally serves to heat the substrate to a moderate temperature (~100°C). Data from table 1 show that anatase is obtained at high *pxd* product (above 500 mm.Pa), that means when particles coming from the target encounter numerous collisions and actually have a low kinetic energy as they imping on the substrate. Thus, if only the energy of the film-forming species is considered, the data reported by Stranak *et al* are in line with the previously reported trends regarding the evolution of phase composition of TiO_2 films with the energy input. In this work, contrary to what was found out by Mráz and Schneider, it appears that the crystalline phase is rather determined by

the kinetic energy of the condensing species than by the total energy transferred during the deposition process.

Thus, these studies point out that, the total energy flux (or the NEF), the carriers of energy flux (metal ions, gas ions, electrons etc.) and their level of contribution to the total flux are key aspects for the phase formation. This is intuitively expected since the same energy brought by condensing atoms that will be converted into mobility at the surface, by incoming species assisting the growth (ions, energetic neutrals etc.) that could cause defect creation, atom displacement, local heating or by electrons, for which probability of momentum transfer is low, etc. will not have the same effect on the growth process. Another illustration of that point can be found in [21, 22]. Petrov *et al.* evidenced that ion-irradiation-induced changes in TiAlN film microstructure, texture, and phase composition follow distinctly different mechanistic pathways depending upon whether the ion energy or the ion/metal ratio was varied (keeping the total energy flux constant). This results in quite different film properties for an identical NEF value.

All the above cited works highlight the interest of performing energy flux measurements in combination with more conventional plasma diagnostics (Langmuir probe, mass spectrometry, etc.) in order to predict, and ultimately control, the film properties.

Beyond the knowledge of the total energy deposited, some energy-related diagnostics tools based on short response time sensors, allow performing real time measurements during the process. This appears a convenient way to monitor the whole deposition process, allowing the detection of any deviation from the normal operation conditions.

The aim of this paper is to illustrate and discuss the interest and limitation of performing energy flux measurements in magnetron sputter deposition experiments. In that purpose, we summarize our recent data but also present new results on the measurement of the energy flux using a thermopile-based diagnostic. The latter will be described in the next section. This kind

of probe, allowing a direct, time-resolved, measurement of the energy transfers can help in partly de-correlating the various energetic contributions at the substrate and, thus, pinpoint the elementary processes of energy transfer. In this article, our experimental data show the evolution of the energy flux at the substrate surface during magnetron sputter deposition when varying working parameters such as sputter power, magnetic field configuration, cathode material, discharge type, gas mixture, etc. We also present results related to the *in situ* oxidation of freshly deposited metal films as well as other experiments which were chosen specifically to distinguish the various energy flux contributions eventually arising during physical vapor deposition processes. In the last section, in light to what has been learnt from the first sets of experiments, the relationship between the energy flux and the film properties is presented and discussed for two specific cases.

2. Quantifying energetic contributions in magnetron sputtering processes.

2.1 Ways to determine the energy transfers at the substrate position

The first way to evaluate the total input power at the substrate during magnetron sputter deposition is to list all the expected contributions and evaluate energy balances. It can be calculated from equation (1) by combining several plasma diagnostics allowing to measure the fluxes and energy distribution functions of plasma species and/or by performing simulation studies of particle-surface interactions that occur at the substrate level.

Even if this method is based on experimental data i.e. the characterization of the gas phase, assumptions must be made. For instance, the energy effectively released by the particles interacting with the surface during condensation, by momentum transfer or chemical reaction, etc, are not always well defined. Consequently, because of imperfectly known conditions, these calculations only provide approximated values of the energy fluxes or of the total transferred energy. This is the strategy implemented by Mráz and Schneider in [19] where ion energy

distribution functions were monitored by energy – resolved mass spectrometry and the ion fluxes were calculated from electrostatic probe data for various discharge conditions. Mahieu *et al.* combined the results from retarding field energy analyzer with that of energy resolved mass spectrometry and simulations using the SIMTRA code [23, 24] to calculate the momentum flux per incoming metallic particles.

However, to avoid making assumptions when species interacting with the substrate are not well defined, energy transfers can be determined by direct measurements using dedicated probes. With such probes, the total input power at the substrate can be monitored throughout the process. There are different ways to determine the total energy flux incoming at the probe surface: 1) recording the temperature time evolution during heating and cooling steps, so to speak, studying the rate of temperature change at the probe surface in un-stationary regimes; 2) assuming local equilibrium is reached and measuring the energy propagating by conduction inside the probe, that means by determining a temperature spatial gradient. A last method, called active method, is to maintain the probe at a fixed temperature using a feedback control loop, which allows a direct measurement of the energy input. Energy probes are thus distinguished by their working principle and the temperature sensor used (thermocouples, optical sensors, platinum resistance etc.). Some of them require a data processing step, others allow direct, in real time, measurements. These methods may exhibit various time responses, from seconds to ms, making them suitable for different applications and deposition environments.

The energy flux probes that have been the most used in low pressure plasmas processes are calorimetric probes. They are based on type principle 1) (see above) and require recording the temperature evolution during plasma ON and OFF periods. The energy flux is then calculated from the derivative of the temperature versus time curve in both steps. The probe heat capacity must be known, which usually requires a calibration procedure. With such probes the global energy transfer is *a posteriori* accessible. One version, designed by H. Kersten's team, based

on thermocouples, has been successfully used in many low-pressure plasma processes [1]. Recently they have shown that placing a shutter between the heat source and the probe allows measuring the plasma species contribution in pulsed processes with a time response of typically several seconds [25]. It is possible to combine the calorimetric probe with a Langmuir electrostatic probe as a function of the substrate bias voltage, hence monitoring the energy deposited by charged particles [26]. Roth *et al.* have developed a calorimetric probe based on a fiber optic sensor [27]. Measurements have been successfully carried out in a tubular plasma downstream reactor and values were compared to those obtained with a conventional calorimetric probe based on thermocouples [28]. Again, the importance of the calibration procedure, necessary to estimate de heat capacity, has been highlighted.

One way to overcome the uncertainty related to the calibration stage is to use active probes, as mentioned above. May *et al.* have used such a probe in low temperature Ar/O_2 plasmas [29]. The input heating power, i.e. the electrical power applied to heat the probe at a given temperature, decreases when the plasma is lighted on, due to the additional thermal load applied on the probe by the plasma species. This probe has thus the advantage to allow direct, real time, measurement with a time resolution equal to about 10 s. Nevertheless, the probe working temperature should be chosen wisely, depending on the range of expected influxes, to get the proper sensibility.

Energy flux probes based on the second working principle like heat flux transducers, also called radiometers, have been used in plasma processes as reported in [7]. The thermal gradient created between two thermoelements by the incoming heat flux generates an electric potential difference proportional to the magnitude of the heat flux (Seebeck effect), which is then recorded. These kinds of sensors exhibit a short response time, below one second. They require simple calibration to relate the delivered voltage to the incoming energy flux. Ellmer *et al.* have developed a Gardon type sensor especially dedicated to measurements in magnetron sputter

deposition [30]. In their configuration, the radial gradient temperature (between areas exposed and unexposed to the heat flux) is followed. It is calibrated with the help of an argon ion laser beam and after having added a black paint of known absorptivity onto the sensor. They studied the energy flux density at the substrate depending on the target material, the input power, and the magnetic field configuration.

Thermopiles are also based on the Seebeck effect and composed of thermocouples set in parallel or series. they can be used to measure temperature gradients and thus follow the energy flux density in low pressure plasma processes. Such an energy flux diagnostic has been developed at the GREMI laboratory based on a heat flux microsensor commercialized by Vattel (Vattel-HFM-7) composed of a thermopile for the energy flux measurements, and a resistance temperature detector (Pt100) for the temperature control [31, 32]. The thermopile actually consists of an array of 1600 thermocouple junctions per cm^2, ensuring a sensitivity of the order of 1 mW/cm^2. Its active area (6 mm in diameter) is covered by a black paint (of known absorptivity). The intrinsic time response is 300 µs thanks to the thin film design of the metal junctions. Main features and details can be found in [31]. The diagnostic is calibrated according to a NIST protocol with a home-made cylindrical black body satisfying specifications to ensure an emissivity close to 1 [33]. This calibration procedure is performed in a dedicated vacuum chamber. The temperature of the buried metal junctions is maintained at 278 K by a proper cooling circuit. Previous works have demonstrated that the measurements performed in these experimental conditions are accurate and in very good agreement with calculations from energy balances or results obtained with a calorimetric probe [31, 32; 10]. A 100 µm-thick copper foil used as substrate is pasted on the HFM active area using a vacuum-compatible thermal silicone paste. This paste was previously found to ensure a good thermal contact (thermal conductivity of 4.1 $W\ m^{-1}\ K^{-1}$) between the sensor and the copper foil back side so that lateral energy flux losses were avoided [31, 32]. Moreover, because the internal temperature of the HFM is

maintained at 278K during the experiments, the heat flux lines are oriented towards the sensor active surface. The presence of the copper substrate affects the time to reach the local equilibrium and only influences the time response of the system; the latter is degraded down to 500 ms.

Energy flux probes exhibiting response time less than one second and allowing real time measurements have been successfully developed and employed to investigate magnetron sputter deposition processes. They allow monitoring and controlling the whole process, permitting detection of any drifts during the experiment. As mentioned above, they also give some fundamental insight into the elementary mechanisms involved during film growth. Even if the detected signal is the sum of all the energetic contributions at the probe surface, it is possible, in some cases, by properly varying the working conditions, to isolate some of them.

2.2. Detecting low energy contributors: gas conduction

In every low-pressure plasma process, the working gas (typically argon) injected into the vacuum chamber gives (or takes) energy to the substrate by conduction. This low energy contribution, due to physical interaction between the gas atoms and the probe surface, can be detected by thermopile-based diagnostics. To illustrate the capability of such a sensor, measurements were performed using two inert gases, helium and argon, characterized by different thermal conductivities. The corresponding energy flux densities are displayed on the graph of Fig 3 for Ar and He as a function of the pressure.

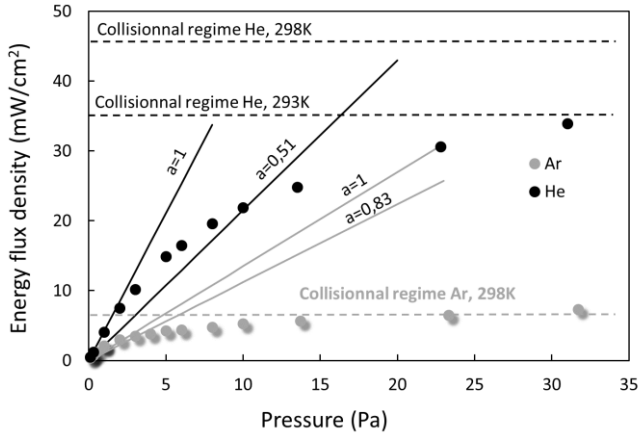

Fig. 3. Energy flux density due to gas conduction measured with a thermopile based diagnostic for Ar (grey) and He (black) gases at various pressures. The sensor temperature was fixed at 278 K. Values calculated for both gases in the so called free molecular (continuous lines) and collisional (dashed lines) regimes are also given for a gas temperature of 298 K. The corresponding value at 293 K for He in collisional regime is also indicated. Accommodations coefficient values are 0.83 and 0.51 for Ar and He, respectively.

It is well known that the regimes of conduction are related to the ratio between the atom mean free path and the probe dimension [34]. When the mean free path of the atom λ_g is much less than the probe diameter, the heat flux density is proportional to the gas thermal conductivity and the local gradient of gas temperature. The regime is collisional and the heat flux brought to the probe can be written as [34]:

$$P_{cond,collisional} = N_u k \frac{T_g - T_S}{2a} \text{ (eq. 2)}$$

where T_g is the gas temperature outside the boundary layer which has a thickness of about one probe diameter ($2a$), k is the thermal conductivity of the gas (1.6 - 1.8 × 10^{-4} W cm^{-1} K^{-1} for argon [34] and for 14.3 × 10^{-4} W cm^{-1} K^{-1} for helium [35]) which is assumed to be independent

of gas temperature and N_u is the Nusselt number (dimensionless thermal transfer coefficient). For this work, the boundary layer is assumed to be free of any convection around the probe and $N_u = 1$ [34], the probe surface is cooled down to T_s=278K, T_g=298K, and the probe diameter equals 3 mm.

At low pressure, the gas cannot be considered as a fluid anymore and the energy deposited by conduction during this so called free molecular regime linearly varies with pressure and is given by [36]:

$$P_{cond,free\ molecular} = \sqrt{\frac{2k}{\pi M}}\frac{AcP}{\sqrt{T_g}}\left(T_g - T_s\right) \quad \text{(eq. 3)}$$

Where *k* is the Boltzmann constant; *M* is the mass of the gas atom; *P* is the gas pressure and *Ac* is the accommodation coefficient.

The estimation of the expected energy flux density should be handled with care, since the knowledge of the accommodation coefficient on the (copper plate-based) probe surface suffers from uncertainty. Values used for calculations in the present work are 0.83 and 0.51 for Ar and He, respectively. They have been chosen from the study carried out by *Kinslow et al.* [37]. One must note that the gas temperature is also not precisely known in our experimental conditions, 298 K is used, with an estimated uncertainty of ±5 K. Since the sensor temperature is 278 K, this gives a value of ΔP/P of 25 %. . To illustrate this point, values of the conduction calculated in the collisional regime are given for both temperatures for He.

It can be seen from this graph (Fig 3) that the two regimes of conduction are clearly identified for both gases. Estimations carried out in the case of the free molecular regime theory (solid lines) lye below the experimental values, indicating that the true accommodation coefficients are certainly higher than those used in the calculations. This could be related to carbon

contamination of the copper plate surface which can occur during handling the latter. It has been evidenced that such contamination leads to accommodation coefficients close to unity [38]. Nevertheless, expected trends are found when looking at the evolution of the values with respect to the pressure and when comparing Ar and He gases, which have different thermal conductivities. Moreover, the order of magnitude of measured values is in quite good agreement with calculated ones for both gases.

Regarding magnetron sputtering processes, these measurements show that in conventional conditions (argon gas, pressure lower than 5 Pa) the conduction contribution on a cold surface (the probe is cooled at 278 K) is low, not more than several mW/cm^2. Moreover, deposition is usually carried out at room temperature, meaning that no energy transfer occurs between the gas and the substrate surface, which are at the same temperature. However, it is known that the temperature of the substrate surface slightly rises during the deposition process and becomes higher than that of the Ar gas. Typical reached values are around 400 K. In this situation, the energy transfer is reversed, and the gas flow induces the cooling of the heated surface. A rough estimation obtained from equation 3 gives values of the order of magnitude of 30 mW/cm^2, which is not negligible. To perform energy flux measurements with the thermopile sensor in magnetron sputter deposition processes, the conduction contribution (heating source in this case) is substracted by calculating ΔJ between plasma ON and plasma OFF signals. But the cooling effect induced by gas conduction in "real conditions" cannot be determined. One has to keep in mind that such a diagnostic allows to probe the energetic contributions at the substrate location, but does not mimic the deposition process itself; the energy balance, that ultimately determines the temperature of the substrate surface, is not reproduced.

2.3 Evidencing chemical reactions at the surface

Another kind of energetic contribution that could be interesting to study is related to chemical reactions taking place at the surface such as oxidation. This is especially relevant for reactive magnetron sputter deposition experiments where a reactive gas such as nitrogen or oxygen is admixed to the argon gas. To explore the ability to detect this kind of contribution, freshly sputtered titanium films were submitted, *in situ*, to molecular oxygen at various pressures (0.2 to 1.6 Pa) in the same vacuum apparatus. The corresponding energy flux measurements are displayed in Fig 4. The evolution of the energy flux at the film surface is monitored as a function of time.

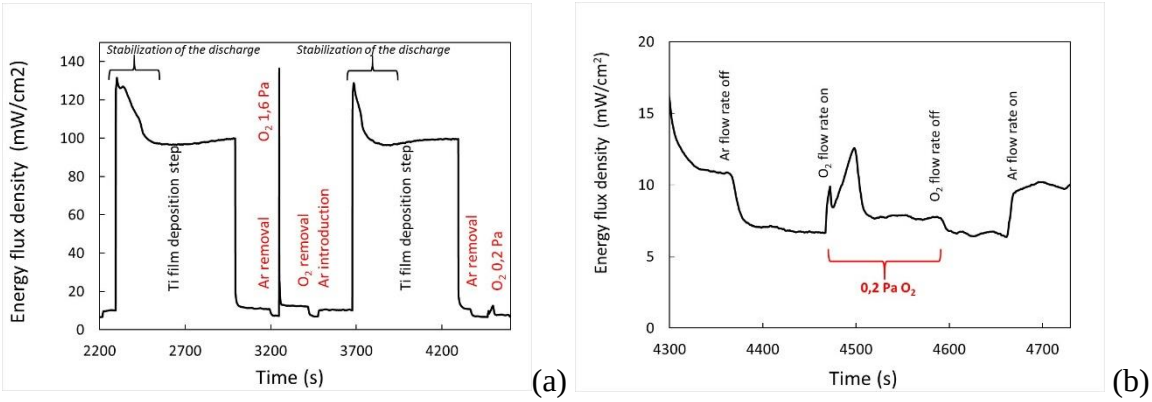

Fig. 4. (a) Energy flux density measurements performed with a thermopile based diagnostic during a run of experiments including Ti film deposition steps (2 Pa Ar pressure, 170 mA, 10 min) and oxidation steps in different oxygen pressures (0.2 and 1.6 Pa). (b) Zoom on the oxidation step under 0.2 Pa oxygen pressure.

The 10 min long Ti deposition steps, carried out between 2300 and 2900 and 3700 and 4300 seconds, are clearly visible. The deposited energy corresponds to the contribution of all the plasma species, including the condensation of the metal atoms. The energy flux peaks, observed as the plasma is lighted ON, are due to the evolution of the discharge during the first minutes

of operation. This effect is attributed to the removal of the oxide layer present on the titanium target while the discharge is driven in the current-regulated mode in this experiment. After this peak, the energy transfer stays almost constant during the deposition step (about 100 mW/cm^2), showing that the sputtering and deposition conditions remain stable. After the plasma was turned OFF, the Ar gas was removed from the chamber (at 3200 and 4380 s, respectively) and oxygen was introduced (at 3300 and 4450 s, respectively) at different pressures (1.6 and 0.2 Pa). A zoom between 4300 and 4700 s given in Fig 4b. The latter shows that each step is clearly detected: i) a decrease of the energy flux (3.8 mW/cm^2) that occurs when the argon flow is stopped (4380 s) and corresponding to the disapearance of the conduction contribution of this gas, then ii) a peak that is observed when oxygen is introduced in the chamber (titanium has a great affinity for oxygen) followed by iii) a steady state. The first peak is attributed to the energy released by the oxidation of the 600 nm thick metallic film. Saturation is reached when the film gets covered by a stable native oxide layer (passivation). At this latter stage, the interaction between oxygen and the passivated surface only happens through gas conduction (iii, the steady state). It is also seen on this graph that the amplitude and kinetics of the energy deposition vary as a function of the oxygen pressure.

To evidence this point, the energy flux peak due to oxidation of a titanium film is presented in Fig 5 for various oxygen pressures. The energy flux density displays an intense and short peak at 1 s only for the 0.5 Pa conditions. This peak is followed by a broader peak centered at 20 s. The first intense peak is not visible for other oxygen pressures and the broad peak lasts longer when the oxygen pressure is low. The maximum of energy related to this second wave of energy decreases from 11 mW/cm² for an oxygen pressure of 0.5 Pa to 3 mW/cm² for 0.14 Pa. Finally, the total amount of deposited energy density obtained by integrating the whole peak (not shown here) decreases with the pressure of oxygen. Dependence of the oxidation kinetics and the total

energy deposited with the pressure agrees with what is usually reported on the oxidation of metals, and especially regarding the oxidation of titanium surfaces [39, 40].

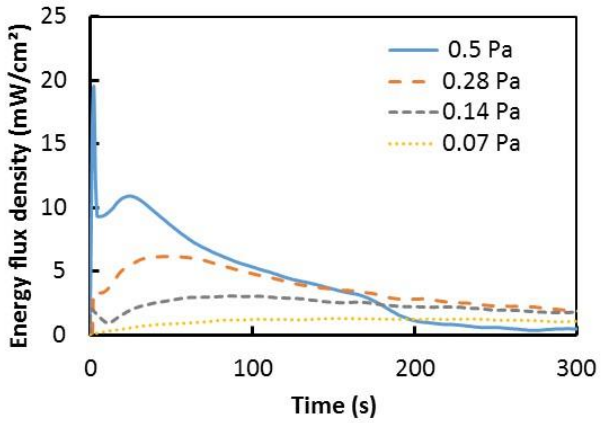

Fig. 5. Energy flux density measured with a thermopile based diagnostic during the interaction of freshly deposited 600 nm thick titanium films (150 W, 10 min, 4 Pa) with oxygen at various pressures.

2.4 Radiations from the hot target surface and related phenomena.

It has been proved in a previous study that using a thermopile sensor could allow separating contributions of the plasma species from those due to thermal processes [16]. The latter are characterized by much slower kinetics. The gradual heating of the sputter target surface can be therefore evidenced. This is illustrated in Fig 6 where measurements are performed in front of a nickel target in two experimental configurations: the first one ensures an efficient cooling of the target and is referred to as the ”cold target” configuration while, for the second one, the thermal contact between the sputter target and the cooled cathode body has been intentionally weakened by the addition of a ceramic MACOR® disk having a low thermal conductivity (1.46 W m^{-1} K^{-1}). This situation is referred to as the “hot target” configuration.

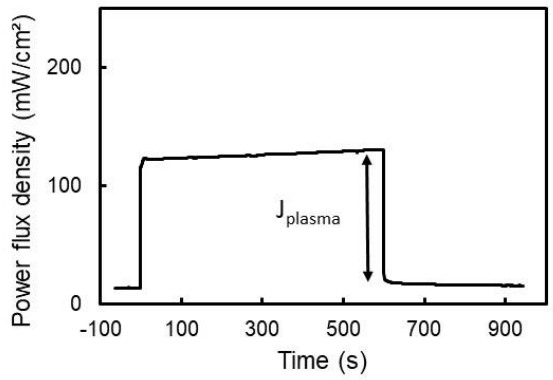

(a)

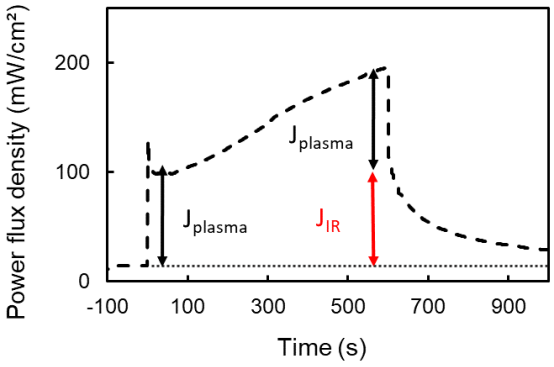

(b)

Fig. 6. Energy flux density measurements above a nickel target DC-sputtered at 100 W in "cold target" (a) and in "hot target" (b) configurations. The contribution from the hot target emitting IR photons (J_{IR}) and the contribution arising from plasma species (J_{plasma}) are highlighted (respective red and black arrows).

In the "cold target" configuration, the signals exhibit a top hat-shaped waveform i.e. a sharp increase (decrease) of the energy flux density is detected when the plasma is lighted ON (OFF) indicating that the only energetic contribution evidenced is that of the plasma species. In the "hot target" case, the same sharp increase is observed at the plasma ignition (J_{plasma}), but a slow increase is then observed after several minutes of running the plasma ($J = J_{plasma} + J_{IR}$). Just after the plasma extinction (600 s), the J_{plasma} is null and J_{IR} (red arrow) can be measured. The kinetics of this IR contribution is typical of a thermal process. The temperature of the target

surface, which is submitted to an intense bombardment by plasma ions, increases. In turn, the hot target emits infra-red (IR) photons following a grey (emissivity < 1) body radiation law that are collected by the probe set in front. This phenomenon has been specifically studied in [41]. This IR contribution also exists even in conventional magnetron sputtering conditions but it is usually small and therefore ignored. This contribution can vary a lot between studies because it strongly depends on the target characteristics such as thickness and thermal conductivity but also on technical details like cooling circuit and cathode design (direct or indirect cooling), the target clamping, etc.

From the IR radiation contribution (J_{IR}), using the Stefan law, and assuming a mean emissivity value of the target and the HFM surfaces, it is possible to estimate the target surface temperature. For some target materials, the emissivity could be estimated at some specific temperature thanks to the presence of physical phenomenon such as the transition between ferro-magnetic and non-magnetic states for nickel (358°C) [41] or the α-to-β phase transition for titanium (882°C) [42]. Another way is to combine radiative measurements (IR camera, pyrometer, thermopile) to the determination of the temperature evolution performed with a thermocouple embedded at the target backside. Such evaluation of the emissivity assumes that the thermal conductivity of the metallic target is generally largely superior to the thermal conductivity of the ceramic spacer disk (in hot target configuration) and so temperature gradients inside the target are negligible. Fig. 7 gives an example of the emissivity of a 2 inches aluminum target (ε_{target}) along its diameter obtained by combining thermocouple and IR camera measurements, 0 mm corresponding to the center of the circular target. In the racetrack submitted to intense ion bombardment and sputtering, between 5 and 13 mm, the emissivity appears to be much lower, i.e. close to 0.1, than in the center and the sides where re-deposition mainly takes place. The measured emissivity is thus close to the value of a polished metal inside the racetrack and to that of a rough oxide surface elsewhere.

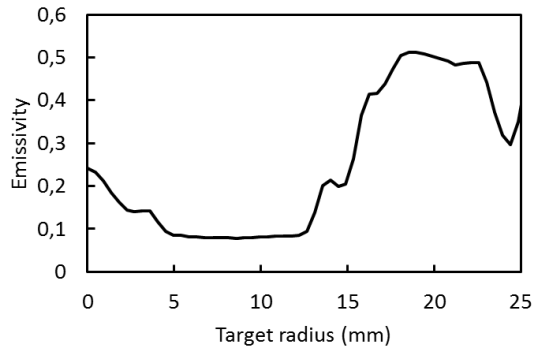

Fig. 7. Emissivity of a two-inch aluminum target estimated after 15 min of sputtering at 500 V by combining IR camera and backside thermocouple measurements. The temperature of the target is assumed to be homogeneous over the whole surface. Al thermal conductivity is about 210 W m^{-1} K^{-1}.

Considering the circular geometry of the target, it has been possible to estimate a mean value of the target surface emissivity ($<\varepsilon_{target}>$ = 0.3 from Fig 7). From there and using the thermopile sensor, the evolution of the surface temperature during the sputtering process of an aluminum target can be calculated. In this respect, and to avoid superimposing the plasma contribution, the plasma was sequentially turned OFF for 1 - 2 s during the sputtering step to solely detect the IR radiation (J_{IR}) emitted from the target (see Fig 8a). The target temperature can be sequentially calculated from the energy values corresponding to the IR radiation. Example of typical results are presented in Fig 8b for the sputtering of a two-inch aluminum target thermally disconnected from the cooled cathode. Working at 65 W, the temperature reached 480 °C after 10 min.

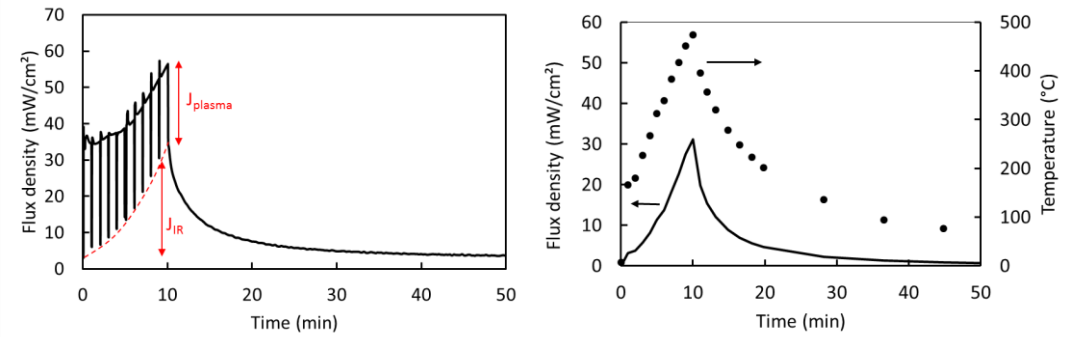

(a) (b)

Fig. 8. a) Energy flux density evolution during the sputtering of an aluminum target sputtered with a power of 65 W in "hot target" configuration. The plasma is switched OFF after 10 minutes. During the sputtering ON step, the plasma is sequentially stopped to measure the IR contribution (J_{IR}). b) Corresponding evolution of the IR contribution and of the target surface temperature evaluated using the Stefan law from the IR contribution. A mean emissivity was experimentally determined ($<\varepsilon_{target}>=0.3$) and the mean absorptivity of the Ni thin film on the HFM was assumed to be also 0.3.

In "cold target" configuration, the surface temperature of a titanium target can also be increased through ion bombardment. Cormier *et al.* [16] used the energy flux data and the Stefan law to estimate the target temperature in DC and HiPIMS regimes. The temperature is surprisingly high and rises from 210 up to 570°C as the power increases from 100 to 800 W for a four-inch titanium target in the DC case. With a balanced magnetic architecture, the temperature increase is enhanced because of the confinement of the plasma close to the target (as compared to un-balanced configuration) [16]. This trend is furthered if an HiPIMS plasma is produced in the same balanced magnetron setup and a temperature of 870°C is reached for a sputtering power of 400 W. In this latter case, noteworthy, more than 75% of the energy deposited on the substrate is due by IR photons emanating from the hot target. These results show that even in "cold target" configuration, the target temperature could be significantly increased and the

energy flux coming from the IR radiation could be much larger that the energy coming from the plasma sputtering process itself. Of course, such result greatly depends on the sputtering conditions such as the sputter power, the magnetic field configuration, the thermal contact between the target and the cathode, the cooling efficiency of the magnetron head, etc. It was observed that with the addition of a copper foam (purchased from Neyco, thermal conductivity of about 370 W m^{-1} K^{-1}) between the target and the magnetron, the thermal conductivity of the whole system is substantially improved and the heat is efficiently evacuated leading to a decrease of the target surface temperature.

From the above results, it appears that direct measurements of the energy flux density may be a convenient way for real time monitoring, including the detection of any change in the sputtering and film growth regimes, and therefore allowing the control of the whole process. It is also possible to get an insight into the target temperature. Besides these aspects, studying the IR radiation emitted by the heated target is of relevance for the thin film growth itself since it has been reported that this contribution may have an influence on the film characteristics [43-45]. Tracking the target temperature increase is of interest in "hot target" sputtering configuration when the target is intentionally disconnected from the cooling system in order to induce the ejection of target material by coupling evaporation to sputtering. This is a way to achieve high deposition rates in the case of elements exhibiting low sputtering yields, or to modify the spatial homogeneity of the chemical composition in alloy thin films [46, 47, 48].

2.5. Plasma contribution

2.5.1. Non-reactive magnetron sputtering

Obviously, the way the plasma is generated affects the energy flux deposited on the substrate surface. In this section, we first discuss the results obtained during non-reactive plasma e.g. when only argon gas is introduced into the vacuum chamber to synthesize metallic films.

It is known from plasma diagnostic studies that an increase of the input power leads to the formation of a denser plasma, with an increase of the electron/positive ion density, and increases the number of sputtered atoms. This situation leads to an augmentation of the total energy flux at the substrate location. Here, energy contributors are, as highlighted by eq. 1 and further discussed in [1], film-forming metal atoms (including condensation enthalpy and kinetic energy), plasma ions (Ar^+), metastable argon atoms, (fast) neutrals, electrons, and photons emitted by excited plasma species as well as IR emanating from the heated target. Depending on the experimental conditions, such as target to substrate distance, argon pressure, substrate bias voltage etc., relative contributions of these species vary. Drüsedau et al proved that the mass of the target element could also play an indirect role because it will influence the reflection rate of argon ions [49]. Argon ions are accelerated through the target sheath, eventually neutralized, and reflected back towards the substrate. In their work they highlighted that such reflected neutrals bring a large part of the deposited energy at the substrate when heavy elements are sputtered by low kinetic energy ions. This has been evidenced by other authors [11, 49-51]

In Fig. 9 [16], plasma and IR contributions are plotted as a function of the input power in the case of DC sputtering of a titanium target ("cold target" configuration with a balanced magnetic field). It is seen that the plasma contribution linearly increases with the sputter power, whereas the IR one rises exponentially and therefore plays an increasingly role on energy deposition at the substrate for large input power conditions.

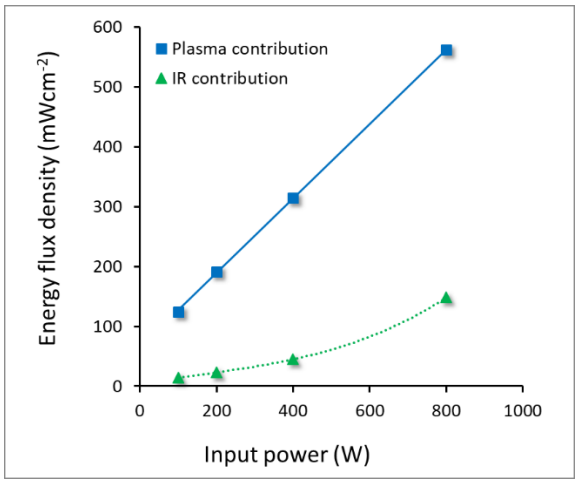

Fig. 9. Influence of the cathode power on the energy flux density (plasma and IR contributions) at the substrate during DC magnetron sputtering process of a 10-cm in diameter Ti target, at 0.66 Pa argon pressure [16].

The influence of the working gas pressure on the global energy influx ($J_{plasma} + J_{IR}$) is displayed on Fig 10 in the case of a 10-cm circular titanium target in various sputtering discharge regimes: Unbalanced DC, pulsed DC, High-Power Impulse, and Balanced DC magnetron sputtering.

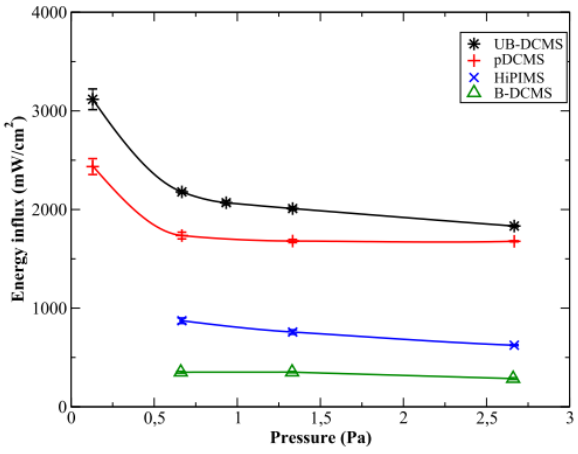

Fig 10: Influence of the working gas pressure on the energy flux at the substrate position displayed for various types of sputtering discharges (taken from [15]). These measurements

are performed at the same (time-averaged) cathode power of 400 W applied on a 10-cm in diameter titanium target. For the HiPIMS and pulsed-DC discharges the duty cycle were 4 and 95%, respectively. An unbalanced configuration was used for HiPIMS and pulsed-DC. B stands for balanced while UB stands for unbalanced magnetic architecture~~. The latter have been characterized in [14].~~

The UB DC and pulsed DC discharges could be carried out at low pressures (0.1 Pa). In this condition, sputtered metal atoms are transported in a collision-free regime from the target to the probe and keep their initial kinetic energy which is typically in the range of 2-5 eV. As the pressure is increased (P > 0.5 Pa), gas phase scattering occurs and the kinetic energy of the sputtered atoms is partially transferred to the background gas. In the same manner, the kinetic energy of species assisting the growth like argon ions, fast neutrals, etc. is lowered. Consequently, the global energy flux decreases as compared to the low pressure collisionless regime. The energy flux decreases asymptotically with the pressure and reaches a minimum for pressure around 1.5 – 2.5 Pa.

Working with an unbalanced magnetic field allows guiding the secondary electrons towards the substrate holder and intensify the bombardment of the growing film, e.g. by argon ions. It is well documented that the ion current at the substrate surface increases significantly in this situation [52]. Such unbalanced configuration should enhance the energy flux density deposited on the substrate. Such hypothesis has been confirmed in the literature using different sensors. In DC regime, using the thermopile sensor, Cormier *et al.* have shown that unbalanced configuration induces a five-fold increase of the energy flux as compared to the balanced configuration, as shown figure 10 or in [16].

High-Power Impulse Magnetron Sputter (HiPIMS) deposition processes were developed to increase the ionization degree of the metal atoms. In such a process, metal ions which can be

sometimes multiply ionized are found to have an energy distribution function extending to higher kinetic energies as compared to DC magnetron discharges, as reported in numerous papers dealing with mass – energy analysis of these pulsed plasmas [53 and references therein]. Nevertheless, from Fig 10 above, it is found that the energy flux is surprisingly low for HiPIMS discharges obtained in unbalanced configuration when compared to an unbalanced DC regime. To explain this trend, one has to remind that even if ions with high kinetic energies are evidenced in HiPIMS discharges by mass spectrometry, for instance, their flux, which is difficult to quantify, might be rather limited. This results in quite low NEF values as found here for an HiPIMS discharge: 1480 eV/at at 0.66 Pa. For the DC and pulsed DC discharges, the NEF equals 2480 eV/at and 1900 eV/at, respectively. Moreover, in this study the HiPIMS regime was characterized by a rather low peak power density (132 W/cm^2 for a duty cycle of 4% and a mean power density of 5.3 W/cm^2). Such observation has also been reported elsewhere using calorimetric probes [53, 54] where the HiPIMS discharge was ignited on a 10 cm in diameter titanium target at 1.6 Pa, and at a relatively low voltage and peak current (~500V – 30 A) hence producing a rather low peak power density (200 W/cm^2), and most likely a relatively reduced ionization degree of the metallic vapor. In this last reference, the energy flux density normalized by the deposition rate (expressed in mW/cm^2/(nm/s)) is 2 and 8 times lower in HiPIMS than in DC and pulsed-DC regime, respectively, in agreement with the present results. In the case of HiPIMS discharge operating at higher peak power densities, the contrary is observed. In the study of Leroy *et al.* [55], where a calorimetric probe was used, the HiPIMS discharge (~4500 W/cm^2 peak power) delivers 1.5 - 3 times more energy per depositing particles than the DC metallic mode. In this situation, the deposition rate is lower in HiPIMS mode than in DC mode whereas the energy flux densities were found to be comparable in both modes.

Thus, from the above examples, it appears clearly that no universal trends can be drawn on the energetic conditions at the substrate depending on the kind of sputter discharge used. Even in conditions where highly energetic particles are expected, the total energy flux density may be relatively moderate. This highlights the need of carefully setting up the deposition process to control the energy deposition. Also, coupling direct measurements of the energy flux density to detailed diagnostics of the gas phase can be useful to understand what are the species involved in energy deposition while keeping in mind that no plasma diagnostic allows to detect every plasma species. Plasma diagnostics alone can hardly prioritize the species and even quantify the energy effectively deposited at the substrate. Careful investigation is needed to properly qualify the energetic conditions (total energy transfer and highly energetic species) and to correlate them with the deposited film properties, as it will be illustrated in section 3.

2.5.2. Reactive magnetron sputtering

Highlighting the so-called transitions regime

In reactive conditions, the sputtering regime changes from metal to compound one as the reactive gas flow rate increases and a critical value of the reactive gas partial pressure is reached. This phenomenon has been studied for a long time, for example in the case of the synthesis of oxide or nitride metal compounds, and is today relatively well understood [23, 55-57]. A way to evidence the transitions is to follow the evolution of the target voltage or/and of the pressure inside the chamber with respect to the reactive gas flow rate. Since the energetic conditions at the substrate are expected to vary significantly in metal and compound regimes (modified sputtering plasmas and gas phase composition), studying the energy transferred to the substrate when the reactive gas flow rate varies should also allow evidencing the transition. This is illustrated in Fig 11 in the case of a 4-inch titanium target sputtered in Argon/Oxygen mixture at 400 W. The energy influx (in mW/cm^2) in this figure is obtained by subtracting the

IR contribution (according to the procedure described in Figure 8) and corresponds to the contribution arising from the plasma species (J_{plasma}). This is possible by performing step by step measurements, as reported in [58]. Some key features can be extracted from Figure 11. First, there is a bump in the energy flux before the dramatic reduction of the energy flux observed at 15 % O_2 flow rate accompanied by the decrease in deposition rate (not shown). This bump is due to the getter effect i.e. the reaction of oxygen with the titanium metallic film which is growing on the probe surface (same process than that described in section 2.3). In the present case, the release of the energy due to the formation of the metal – oxygen bound was found to be proportional to the amount of chemical bounds formed and to the enthalpy of formation [14]. The energy released equals 570 mW/cm^2 in the present situation.

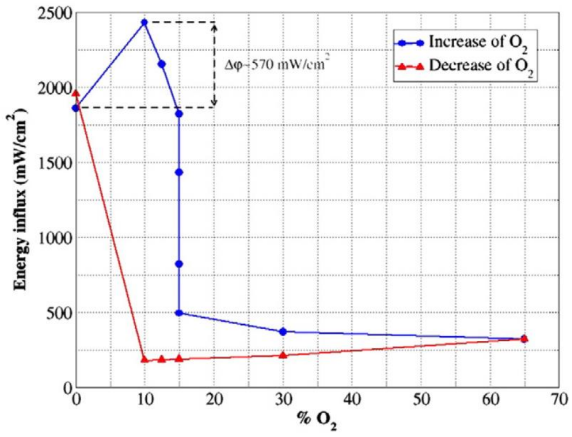

Fig. 11. Evolution of the energy flux density (plasma contribution) at the substrate as a function of the oxygen partial flow in the case of titanium reactively sputtered in an Ar/O_2 atmosphere (DC discharge, 400 W, 0.6 Pa) (taken from[14]).

Second, the sharp decrease (increase) of the energy flux observed at 15% (10%) seems to correspond to metal/oxide and oxide/metal transitions. To check this point, comparison with the evolution of plasma parameter exhibiting the well-known hysteresis behavior has to be done.

On figure 12, the target voltage and the energy flux are plotted for different sputter powers (50, 100 and 150 W on a 2 inch Ti target)); one can see that the metal-to-compound and compound-to-metal transitions are spotted by the appearance of an energy peak. In these experiments, however, the oxygen flow rate was continuously increased and then decreased at a rate of 0.5 sccm/min and the total energy influx is reported ($J_{plasma} + J_{IR}$). Thus, these results cannot be compared to those presented in figure 11. In this kind of measurements, physicochemical phenomena abruptly change as the transition point is reached and influence the energy flux at the substrate position: i) the bombardment of the substrate (or the probe) surface by plasma species (since particles that are sputtered and gas-phase species are different in metal and oxide modes), ii) the ability of chemical reaction to take place (when oxygen atoms are present in the gas phase and oxidize the metallic films), iii) the IR contribution of the target whose temperature rises during the experiment and emissivity changes significantly depending on its surface state, etc. Consequently, a complete interpretation of the features of these curves (presence of bumps at transitions) is rather difficult. Nevertheless, when analyzing Fig 12, it appears that these peaks, associated to the transitions, are shifted towards lower (higher) oxygen flow rate values when the input power is decreased (increased). This is in good agreement with what is expected: since at lower power the sputtering process is less efficient, poisoning (cleaning) of the target occurs for lower (higher) oxygen flow rates.

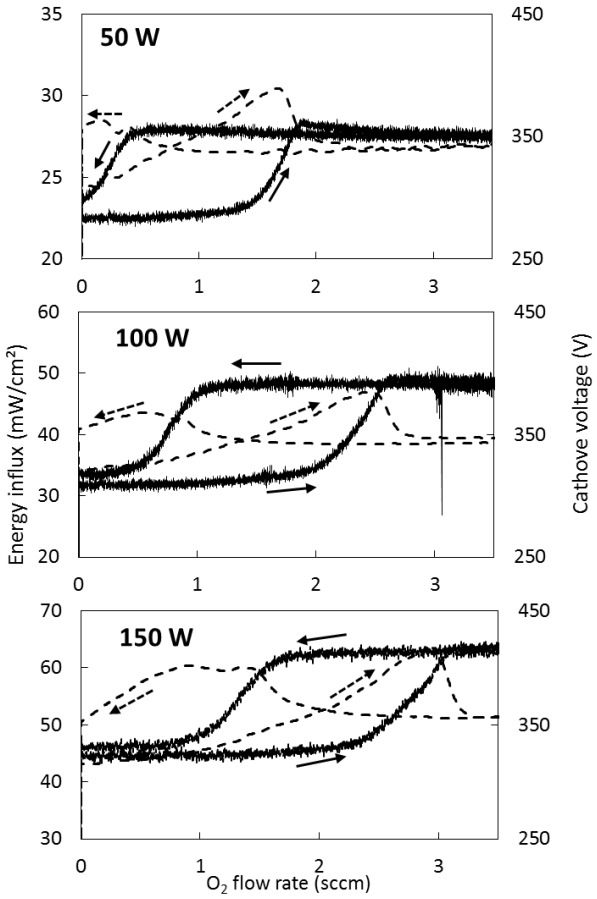

Fig. 12. Evolution of the total energy flux density (dashed lines) and the target voltage (full lines) for various powers (50, 100 and 150 W for a 2 inch Ti target) when the oxygen flow rate is increased and then decreased at a rate of 0.5 sccm/min (indicated by the arrows).

Finally, one can track, thanks to the energy flux, the well-known hysteresis behavior which is obtained when increasing and then decreasing the oxygen flux. These observations emphasize that the energetic conditions at the substrate significantly vary as the sputtering/deposition regime is modified. Following the energy flux at the substrate may be a convenient way to monitor the deposition process.

Energy deposited in oxide mode

In the case of Ar/O_2 plasmas, as the process enters the poisoned regime, it is known that the target chemistry and plasma composition change, modifying the plasma/substrate interaction [54]. The ion-induced electron emission yield of the target surface varies and metal compound molecules as well as negative oxygen ions are emitted. Those negative oxygen anions, or other negatively charged ions [59, 60], are accelerated in the target sheath in which the potential is typically in the range of a few hundreds of volts and is close to the applied discharge voltage. Consequently, very fast negative ions enter the plasma and bombard the substrate. Mráz *et al.* proposed that the formation of nanocrystals for transition metal oxide films deposited at room temperature is induced by those oxygen anions [61].

The variation of energy flux measured as the magnetron discharge enters the reactive mode was discussed in [14] and was also linked to the emission of fast negative ions. Indeed, the deposition rate was, as usually observed in this case, significantly decreased while, to the contrary, the NEF increased from ~4500 eV/at up to ~11 000 eV/at as the target surface became poisoned. These values are in line with those previously reported by Thornton [11], Drusedau [12], and Leroy *et al.* [55].

If a High-Power Impulse Magnetron Sputtering discharge is operated in a reactive mixture, the NEF is even further augmented [14]. In this case, three effects are combined in producing very large NEF values as the discharge enters the poisoned regime. It is known that the deposition rate in HiPIMS is reduced as compared to DC processes carried out at the same sputter power. As mentioned, concomitantly, the target voltage and peak current are larger in HiPIMS processes as compared to DC magnetron plasmas. As a result, the metal atoms are efficiently ionized, and their kinetic energy is increased (see [62] and references therein). In this situation the target sheath voltage is also augmented and the kinetic energy of the negative oxygen ions emitted from the target surface reaches extremely large values i.e. several hundreds of volts higher than during the DC-magnetron counterpart [63].

Because of the large metal ion fraction in the deposition flux, the magnetic configuration is an important parameter in HiPIMS technology [64, 65]. This effect was also observed in reactive discharges. A HiPIMS discharge run in Ar/O_2 mixture at a time-averaged power of 800 W, with an unbalanced magnetic field (when the magnetic field lines steer the dense metal ion cloud towards the substrate), allows reaching a NEF as high as 45 keV/at while, in the same conditions, an equivalent DC plasma delivers 7 keV/at [14].

Energetic contributions in oxide mode

As shown before, in the section related to non-reactive sputtering, particles carrying the highest kinetic energies may not be the main ones responsible for the increase of the NEF. In the complex case of reactive sputtering, coupling energy flux measurements with other diagnostics like energy-resolved mass spectrometry can further improve our knowledge of the plasma/surface interaction process [66]. Many different species can interact with the growing film in this case since oxygen-containing particles can be ejected from the poisoned target and/or created in the plasma, whose chemistry has completely changed due to the presence of oxygen that is no longer consumed inside the chamber.

In the case of aluminum sputtered in Ar/O_2 mixture the detected species are typically O^-, O_2^-, O^+, AlO^+, AlO_2^- and AlO^-. Among them, as mentioned above, O^- has been reported to play an important role in the energy transfers and different populations have been identified depending on their kinetic energy [58].

Figure 13a displays the typical energy distribution measured by the energy-resolved mass spectrometer. Three major ion populations can be observed: low (from 40 to 100 eV), medium (from 60 to 180 eV), and high energy (from 200 to 350 eV) O^- ions with energy corresponding approximately to the negative target voltage. The origin of these peaks has been discussed in the literature [59]. The high energy population comes from the O^- emitted by the cathode and

accelerated through the cathode sheath. The medium energy population originates from the dissociation of O_2^- and AlO_x^- ions (also born at the target), whereas the low energy one may be formed via dissociative electron attachment and subsequent acceleration over a fraction of the target potential. In figure 13a, the O^- distribution is plotted for increasing oxygen flow rates. The maximum of each O^- contribution (especially seen on the high-energy one) is shifted towards ±50V when passing the transitions, in direct relationship with the cathode voltage evolution. From figure 13a, it also appears that the intensity of the O^- peaks are higher in the poisoned mode, which indicates an enhanced flux of this specie to the substrate.

To go further, the energy flux coming only from the O^- ions was estimated from these energy distributions, by integrating the energy-weighted distributions. The result of this calculation is shown on figure 13b. The graph shows that the role played by negative oxygen ions in the energy transfer is furthered and could become significant in the poisoned mode. Thus, it seems reasonable to link the often-reported huge NEF values in this regime to the presence of O^- and more generally to high-energy negatively charged species born at the target and accelerated in the cathode sheath.

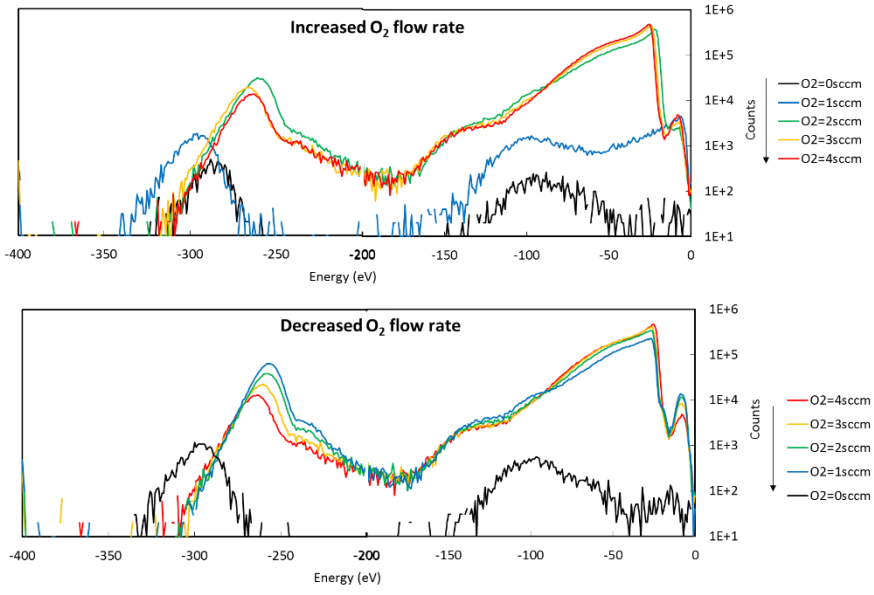

(a)

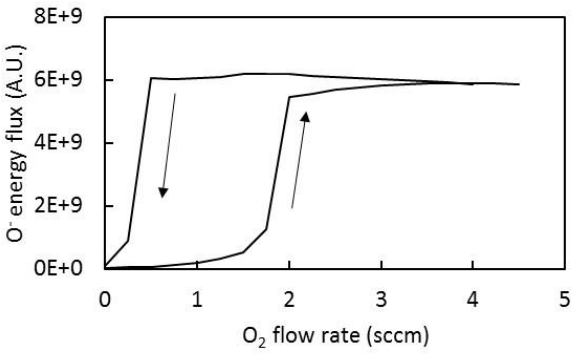

(b)

Fig. 13. (a) Energy distribution of O^- ions measured with an energy resolved mass spectrometer facing the center of a Al target in a mixture of Ar and O_2 gases for increasing oxygen flow rates, (b) energy flux obtained by the integration of the energy distribution between -400 and 0 eV with respect to the O_2 flow rate (DC 100 W, Ar 10 sccm, 1 Pa).

3. Relationship between the energy flux and the crystallinity of metal oxide thin films

3.1. The case of titanium dioxide.

In agreement with what has been reported in the introduction, data collected during the reactive sputtering of TiO_2 films, and previously reported in [13], show that the NEF determines the phase composition of the films which evolves from pure anatase to rutile/anatase-rich mixture, and then anatase/rutile-rich mixtures for further increasing values. These data are reported in

Fig 14 below. For the calculation of NEF both plasma contribution and IR photons emitted from the hot sputtering target (evaluated as in figure 6) have been considered. In this experiment, silicon single crystals with a (100) orientation were used as substrates. They were not heated neither grounded during deposition.

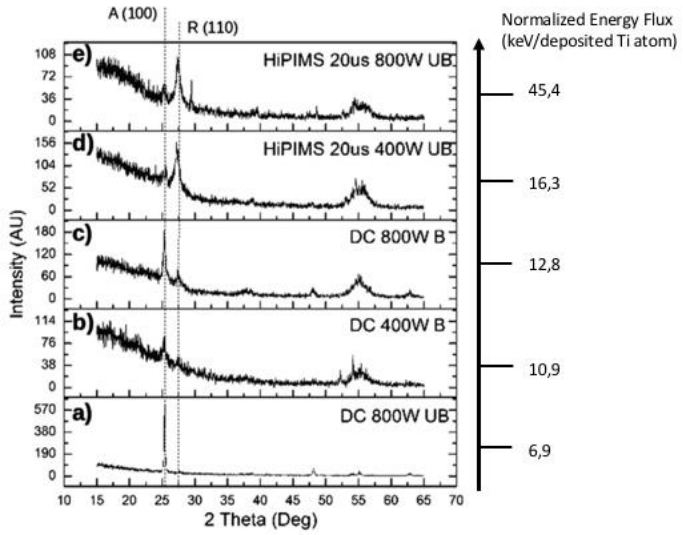

Fig. 14. Phase composition of reactively sputter deposited TiO2 films as a function of the normalized energy flux, as reported in [14]. B and UB stand for Balanced or UnBalanced magnetic field, respectively. Positions of main peaks of anatase (A) and rutile (R) phases are indicated.

The phase composition evolution of the titania films with NEF is similar to what is found in the works of e.g. Löbl [17], Martin [18], and Mráz [19]. However, it should be noticed that if the IR contribution was neglected, the evolution would not have been the same. In the case of the film grown in DC mode at 800 W, despite a higher plasma contribution found with the UB configuration, the total energy deposited at the substrate and the NEF are lower than in the B configuration for which the level of IR radiations coming from the target is large (61 % of the total deposited energy instead of 17 %). This highlights again, as mentioned above, that in B configuration the target is efficiently heated by the dense plasma confined at its vicinity. This

trend is clearly seen on table 2 where highest proportions of IR contributions are obtained with balanced magnetrons as compared to their UB counterparts.

In DC mode at 800 W and with a UB configuration the XRD spectrum is characteristic of an anatase film (Fig 14, diffractogram a), whereas with a balanced magnetic field, for higher total energy transfer, the film phase composition is characterized by a mixture of anatase and rutile (see Fig. 14, diffractogram c). This confirms that rutile requires a higher energy input (or temperature) as presented in the previously quoted articles [17-19].

Table 2 : Plasma, IR radiation contributions, total energy flux, NEF and percentage of IR contribution in various magnetron sputtering working conditions (input power and magnetic configuration) for sputtering discharges operated in the poisoned regime for the deposition of TiO_2 coatings, from [14].

Discharge type	Power (W)	Magnetic Geometry	Energy flux (mW/cm^2)			NEF (keV/Ti at)	% of IR
			Plasma	IR	Total Flux		
HiPIMS	800	UB	682	165	847	45.4	19
HiPIMS	400	UB	223	33	256	16.3	13
DC	800	B	346	548	894	12.8	61
DC	400	B	223	127	350	10.9	36
DC	800	UB	423	88	511	6.9	17

Hence our data highlight the importance the IR contribution when discussing the crystallinity – energy deposition relationship. The other important conclusion is that regardless the working conditions, the NEF is the parameter that allows controlling the phase constitution of TiO_2 films, in a broad range of deposition conditions.

3.2. The case of oxygen-vacancy stabilized zirconium dioxide

In the case of stoichiometric zirconia (ZrO_2), the phase diagram shows that the low-temperature stable phase is the monoclinic one. Above 1200°C, the tetragonal phase is the most stable form and above 2300°C, the cubic phase appears.

In this part of the study, working conditions for the synthesis of non-stoichiometric, oxygen-deficient, zirconia films were carefully devised. The films were grown on floating Si substrates by reactive magnetron sputtering from an elemental zirconium target while the oxygen flow was controlled in real time by implementing a feedback control loop between the target voltage (which is the finger print of the target coverage i.e. oxidation) and the oxygen inlet valve. This setup allows working in the so-called transition zone located between the metallic regime, in which metallic zirconium films are obtained, and the oxidized regime in which stoichiometric zirconium dioxide films are obtained. By working inside the transition zone, oxygen-deficient ZrO_{2-x} films are deposited, and the amount of oxygen vacancies incorporated inside the material can be adjusted. In this work sub-stoichiometric thin films containing 3 % and 16 % of oxygen vacancies are compared. In [67] the experimental setup is described in further details. Furthermore, by using quantum-chemistry based calculations performed at the DFT level, it is demonstrated that the cubic phase is the most stable crystalline structure as soon as more than 3 at% of oxygen vacancies are introduced in the ZrO_2 lattice. X-Ray diffraction (XRD) combined with elemental composition data are matching very well with the above-mentioned calculation results. This result highlights the importance of material defect chemistry on the film properties, even though the coatings are grown by magnetron sputtering during which kinetic effects may dominate.

A deeper analysis of the results shows that the diffractograms only exhibit cubic peaks as the films are grown at high pressure (1.3 – 2.6 Pa) whatever the discharge current (200, 300 or 400 mA). However, if the pressure is reduced i.e. down to 0.7 Pa, while the discharge is still

operated in the transition zone where oxygen-deficient films are obtained, the diffractogram does not correspond to a pure cubic zirconia phase film anymore. Monoclinic peaks also appear. In the more extreme case for which the current equals 400 mA and the pressure equals 0.7 Pa, although the film is oxygen deficient, the monoclinic (-111) is the most prominent peak. This was not expected since, the films are always produced while working inside the transition zone and are oxygen-deficient. These films, according to quantum chemistry-based calculations should be cubic. However, these depositions conditions are supposed to lead to a higher energy deposition at the substrate. Energy flux measurements were thus carried out and data are reported on table 3, in line with the deposition parameters.

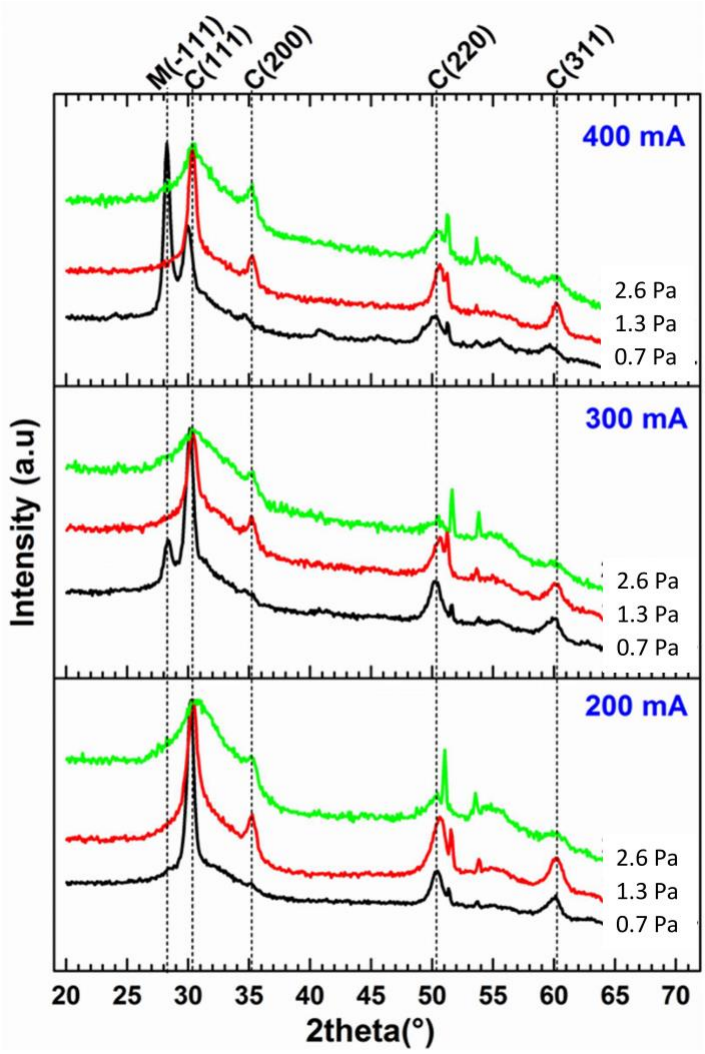

Fig. 15. Evolution of the diffractograms of oxygen-deficient zirconia films (3 % of oxygen vacancies) as a function of the working pressure (0.7 to 2.6 Pa) and discharge current (200 to 400 mA). Peaks labelled M belong to the monoclinic zirconia and those labelled C are related to the cubic phase.

Table 3: Values of the NEF (eV/at) for 16 and 3 at% oxygen vacancy concentrations in zirconia films as a function of the deposition pressure and discharge current.

Current (mA)	***Argon pressure (Pa)***		
16 at.% O Vac			
	0.7	***1.3***	***2.6***
200	1031	598	395
300	1314	762	504
400	1598	927	613
3 at.% O Vac			
200	1313	823	n.a

According to data provided in table 3, a decrease in the pressure and an increase in the discharge current indeed lead to an increase of the NEF. This observation holds whatever the amount of oxygen vacancies incorporated in the material, 3 or 16 at%. This increase in the NEF could be related to the increase of the deposition flux (when the current rises) and of the kinetic energy of the film-forming species as the mean free path increases at lower pressures.

In Fig 16, the phase constitution of the zirconia films, as extracted from the XRD data presented in Fig 15, and the NEF values from table 3 are combined. Zones where oxygen deficient zirconia films are pure cubic phase and where diffractograms are made of cubic and monoclinic peaks can be distinguished. Films grown with a NEF lower than ~1000 eV/Zr atom exhibit a phase pure cubic structure. Above this threshold value, monoclinic peaks are found on the XRD pattern and the intensity of the (-111 peak) increases as a function of the NEF. Although there are no clues why the threshold appears at this value, it can be speculated that effects such as

surface heating, knock-on processes, atom diffusion on the surface, may be enhanced as the NEF increases. This situation leads to a modification of the film growth conditions at the atomic scale which seems to hinder the thermodynamics-based stabilization mechanism of the cubic phase due to the film defect chemistry, as emphasized by quantum chemistry – based calculations.

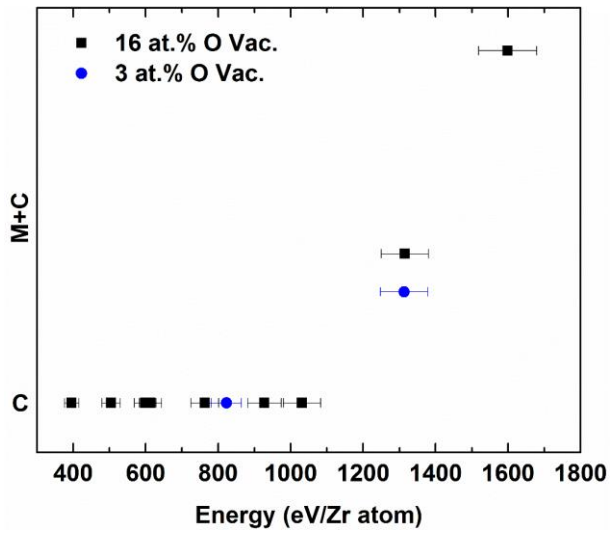

Fig. 16. A "phase diagram" showing the evolution of the phase constitution of oxygen deficient zirconia films as a function of the normalized energy flux at the substrate. Blue data points correspond to film characterized by 3 at% of oxygen vacancies and black markers correspond to 16 at% oxygen vacancy concentration in the zirconia film. Films grown with NEF lower than 1000 eV/Zr atom exhibit pure cubic phase structure.

4. Conclusions

Energy deposition is an important issue in magnetron sputtering processes. Using a thermopile-based sensor allows studying energy deposition during such physical vapor deposition processes with a time resolved capability (ms range) and a quite high sensitivity (mW/cm^2 range). By coupling this tool to a deposition rate measurement technique, the NEF parameter could be estimated. In many cases, it allows to usefully compare deposition conditions, and

predict final film features, like the formation of given crystalline phases, for instance. But, this parameter is not universal and the carriers of energy flux (metal ions, gas ions, electrons etc.) and their levels of contribution to the total flux are key aspects for the phase formation.

Using such a tool, a better understanding of the various contributions arising from magnetron sputtering can be gained; especially separation between collisional and thermal processes can be achieved. IR emission from the gradually heating sputtered target could be evidenced and allowed estimating the target surface temperature reached during the sputtering phase. This contribution is sometimes very large, even when performing HiPIMS depositions during which the ion bombardment at the substrate surface is assumed to be very intense. The knowledge of this contribution is of particular relevance since it could modify the final film properties. This has been illustrated in the case of titania film synthesis, for which the IR contribution must be taken into account to predict the formation of the high temperature rutile phase. Moreover, following the target temperature increase is of particular interest in “hot target” sputtering configuration when the target is intentionally disconnected from the cooling system in order to induce the ejection of target material by coupling evaporation to sputtering.

Other energetic contributions could also be identified like physical interaction or chemical reaction between the gas phase molecules and the substrate. We have shown in reactive magnetron sputtering of a titanium target in argon/oxygen mixtures that chemical reactions take place in the metallic mode when the metal growing film is submitted to oxygen. Since the deposition of compounds, is often carried out in such experimental conditions (close to the metal/oxide transition at high oxygen flow rates) to keep a high deposition rate coupled with the incorporation of a large amount of oxygen inside the film, the detection of this chemical reaction could be of interest for controlling the process.

Even if energy transfer of different kinetics can be separated with energy probes characterized by short response time (thermal transfer, chemical reactions, energy brought by collisions, for instance), only the global deposited energy is accessible. Determining the species playing the main role in energy deposition requires correlating energy flux measurements with the characterization of the plasma and gas phase. Among others, Langmuir probes, retarding field analyzers, and energy-resolved mass spectrometry are tools that can be used to detect the various species interacting with the substrate surface and determine their energy distribution function. We want to emphasize that many reports tend to attribute the modification of the growth process or the final thin films properties to the specie carrying the highest energy. However, the results reported in this article show that, if it is true in some circumstances, this rule is not universal, and measurements of the global energy transferred to the surface is needed to evidence the underlying elementary mechanisms of energy transfer and achieve a complete control on the process.

~~After the metal/oxide transition, many elementary processes bring energy to the substrate surface and their contributions overlap, which makes difficult their detection and identification. Combining such energy flux measurements with other gas phase and plasma diagnostics allow to go further and help evidencing the main species interacting with the substrate and the growing film~~To illustrate the interest of coupling energy measurements and gas phase characterization, we reported the case of aluminum sputtered in an Ar/O_2 gas mixture. Comparing the estimation of the energy brought by O^- ions as deduced from mass spectrometry data with the direct measurement of the energy transfers has allowed evidencing the great role that these energetic species could play when the deposition is performed in the oxide mode.

Beside mass spectrometry, other techniques such as deposition rate measurements with e.g. a quartz microbalance (QMB), can be performed. The QMB can be equipped with a biased electrostatic grid allowing repelling positively charged plasma ions hence allowing

distinguishing the contribution of neutrals and cations. One could also think of electrostatic probes to get a better insight on plasma electrons or even a combination of these three tools for the simultaneous measurements of these plasma parameters, as proposed in [68, 69].

The energy released at the substrate surface is characteristic of the plasma-surface interaction and thus could be used to monitor the plasma treatment, to control the coating properties, and improve the process reliability.

Acknowledgments

SK is research associate of the Fund for Scientific Research (FRS-FNRS, Belgium). SK would like to thank the Walloon Region of Belgium and the European Regional Development Fund for financial support through the Diag&Growth project.

References

[1] H. Kersten, H. Deutsch, H. Steffen, G.M.W. Kroesen, R. Hippler, The energy balance at substrate surfaces during plasma processing, Vacuum 63 (2001) 385

[2] A. Anders, A structure zone diagram including plasma-based deposition and ion etching, Thin Solid Films 518 (15) (2010) 4087

[3] S. Mahieu, P. Ghekiere, D. Depla, R. De Gryse, Biaxial alignment in sputter deposited thin films, Thin Solid Films 515 (2006) 1229–1249

[4] R. Wendt, K. Ellmer, K. Wiesemann, Thermal power at a substrate during ZnO:Al thin film deposition in a planar magnetron sputtering system, J. Appl. Phys. 82 (5) (1997) 2115

[5] H. Kersten, D. Rohdes, J. Berndt, H. Deutsch, R. Hippler, Investigations on the energy influx at plasma processes by means of a simple thermal probe, Thin Solid Films 377–378. (2000) 5 585

[6] D.J. Ball, Plasma diagnostics and energy transport of a dc discharge used for sputtering, J. Appl. Phys. 43 (1972) 3047

[7] R. Gardon, An instrument for the direct measurement of intense thermal radiation, Rev. Sci. Instrum. 24 (1953) 366

[8] J.A. Thornton, Substrate heating in cylindrical magnetron sputtering sources, Thin Solid Films 54 (1) (1978) 23

[9] W.D. Westwood, Sputter deposition processes, MRS Bull. 13 (1988) 6

[10] P.-A. Cormier, M. Stahl, A.-L. Thomann, R. Dussart, M. Wolter, N. Semmar, J. Mathias and H. Kersten, On the measurement of energy fluxes in plasmas using a calorimetric probe and a thermopile sensor, J. Phys. D: Appl. Phys. 43 (2010) 465201

[11] J. A. Thornton J. L. Lamb, Substrate Heating Rates for Planar and Cylindrical-post Magnetron Sputtering Sources, Thin Solid Films 119 (1984) 87-95

[12] T.P. Drüsedau, Kay Koppenhagen, Substrate heating by sputter-deposition of AlN: The effects of dc and rf discharges in nitrogen atmosphere, Surface and Coatings Technology 153 (2002) 155–159

[13] WP Leroy, S. Konstantinidis, S Mahieu, R Snyders and D Depla, Angular-resolved energy flux measurements of a dc- and HIPIMS-powered rotating cylindrical magnetron in reactive and non-reactive atmosphere, J. Phys. D. Appl. Phys. 44 (2011) 115201

[14] P.-A. Cormier, A. Balhamri, A.-L. Thomann, R. Dussart, N. Semmar, T. Lecas, R. Snyders, and S. Konstantinidis, Titanium oxide thin film growth by magnetron sputtering: Total energy flux and its relationship with the phase constitution, Surf. Coatings Technol. 254 (2014) 291–297

[15] P.-A. Cormier, A. Balhamri, A.-L. Thomann, R. Dussart, N. Semmar, J. Mathias, R. Snyders, and S. Konstantinidis, Measuring the energy flux at the substrate position during magnetron sputter deposition processes, J. Appl. Phys. **113** (2013) 13305

[16] P. -A. Cormier, A.-L. Thomann, V. Dolique, A. Balhamri, R. Dussart, N. Semmar, T. Lecas, P. Brault, R. Snyders, and S. Konstantinidis, IR emission from the target during plasma magnetron sputter deposition, Thin Solid Films **545** (2013) 44-49

[17] P. Löbl, M. Huppertz, and D. Mergel, Nucleation and growth in TiO2 films prepared by sputtering and evaporation, Thin Solid Films 251 (1994) 72-79

[18] N. Martin, C. Rousselot, D. Rondot, F. Palmino, and R. Mercier, Microstructure modification of amorphous titanium oxide thin films during annealing treatment, Thin Solid Films **300** (1997) 113–121

[19] S. Mráz and J.M. Schneider, Structure evolution of magnetron sputtered TiO2 thin films, J. Appl. Phys. **109**, 023512 (2011)

[20] V. Stranak, A.-P. Herrendorf, H. Wulff, S. Drache, M. Cada, Z. Hubicka, M. Tichy, R. Hippler, Deposition of rutile (TiO2) with preferred orientation by assisted high power impulse magnetron sputtering, Surface & Coatings Technology 222 (2013) 112-117

[21] I. Petrov, P.B. Barna, L. Hultman, J.E. Greene, Microstructural evolution during film growth, J. Vac. Sci. Technol. A 21 (5) (2003) S117

[22] I. Petrov, F. Adibi, J. E. Greene, L. Hultman, and 36 J.-E. Sundgren, Average energy deposited per atom: A universal parameter for describing ion-assisted film growth?, Applied Physics Letters 63 (1993) 36

[23] S. Mahieu, K. Van Aeken, and D. Depla, in Reactive Sputter Deposition, edited by D. Depla and S. Mahieu Springer, Berlin, 2008, Chap. 6

[24] K. Van Aeken, S. Mahieu, and D. Depla, The metal flux from a rotating cylindrical magnetron: A Monte Carlo simulation, J. Phys. D 41 (2008) 205307

[25] S. Gauter, M. Fröhlich, W. Garkas, M. Polak and H. Kersten, Calorimetric probe measurements for a high voltage pulsed substrate (PBII) in a HiPIMS process, Plasma Sources Sci. Technol. 26 (2017) 065013

[26] S. Bornholdt and H. Kersten, Transient calorimetric diagnostics for plasma processing, Eur. Phys. J. D 67 (2013) 176

[27] C. Roth, G Oberbossel, P Rudolf von Rohr, Electron temperature, ion density and energy influx measurements in a tubular plasma reactor for powder surface modification, J. Phys. D: Appl. Phys. 45 (2012) 355202

[28] C Roth, S Bornholdt, V Zuber, A Sonnenfeld, H Kersten and P Rudolf von Rohr, Comparison of calorimetric plasma diagnostics in a plasma downstream reactor, J. Phys. D: Appl. Phys. 44 (2011) 095201

[29] F. May, S. Hamann, A. Quade, V. Brüser, Study on Cu2S mineral surface modification by low temperature Ar/O2 plasmas, Minerals Engineering 50-51 (2013) 48-56

[30] K. Ellmer, R. Mientus, Calorimetric measurements with a heat flux transducer of the total power influx onto a substrate during magnetron sputtering, Surface and Coatings Technology 116–119 (1999) 1102–1106

[31] A.-L. Thomann, N. Semmar, R. Dussart, J. Mathias, V. Lang, Diagnostic system for plasma/surface energy transfer characterization, Rev. Sci. Instrum. 77 (2006) 033501

[32] L Bedra, A L Thomann, N Semmar, R Dussart and J Mathias, Highly sensitive measurements of the energy transferred during plasma sputter deposition of metals, J. Phys. D: Appl. Phys. 43 (2010) 065202

[33] R. J. Chandos and R. E. Chandos, Radiometric Properties of Isothermal, Diffuse Wall Cavity Sources, Appl. Opt. 13 (1974) 2142-2152

[34] R Piejak, V Godyak, B Alexandrovich and N Tishchenko, Surface temperature and thermal balance of probes immersed in high density plasma, Plasma Sources Sci. Technol. 7 (1998) 590–598

[35] C Normand C. Blais and Joseph B. Mann, Thermal Conductivity of Helium and Hydrogen at High Temperatures, J. Chem. Phys. 32, 1459 (1960); https://doi.org/10.1063/1.1730942

[36] F.M. Devienne, « Low Density Heat Transfer », Advances in Heat Transfer, Volume 2, Academic Press, (1965)

[37] M Kinslow, GD Arney, Thermal Molecular Pressure Effects in Tubes and at Orifices, Arnold Engineering Development Center, AGARDOGRAPH 119, 1967

[38] R. S.Lemons, G. M.Rosenblatt, Thermal Accommodation Coefficients by High Speed Vibration of Solid Samples, Surface Science 48 (1975) 432-448

[39] M. Martin, W. Mader, E. Fromm, Oxidation of iron, aluminium and titanium films in the temperature range 50-200 °C, Thin Solid Films, 250 (1994) 61-66

[40] L. Porte, M. Demosthenous, Tran Minh Duc, Etude ESCA de l'interacion oxygène-titane, J. of less-Common Metals, 56 (1977)183-191

[41] A.Caillard, M.El'Mokh, T.Lecas, A.-L.Thomann, Effect of the target temperature during magnetron sputtering of Nickel, Vacuum 147 (2018) 82-91

[42] J.Tesař, J.Martan, J.Rezek, On surface temperatures during high power pulsed magnetron sputtering using a hot target, Surface & Coatings Technology 206 (2011) 1155–1159

[43] W. F. Yang, Z. G. Liu, Z. Y. Wu, M. H. Hong, C. F. Wang, Alex Y. S. Lee, and H. Gong, Low substrate temperature fabrication of high-performance metal oxide thin-film by magnetron sputtering with target self-heating, Appl. Phys. Letters 102 (2013) 111901

[44] A. Caillard, M. El'Mokh; N. Semmar; R. Dussart ; T. Lecas ; A.-L. Thomann, Energy Transferred From a Hot Nickel Target During Magnetron Sputtering, IEEE transition on plasma science 42(10) (2014) 2802

[45] D. V.Sidelev, M. Bestetti, G. A.Bleykher, V. P.Krivobokov, V. A.Grudinin, S. Franz, A. Vicenzo, Y. L. Shanenkov, Deposition of Cr films by hot target magnetron sputtering on biased substrates, Surface & Coatings Technology **350** (2018) 560-568

[46] D. V. Sidelev, G. A. Bleykher, V. P. Krivobokov, Z. Koishybayeva, High-rate magnetron sputtering with hot target, Surface & Coatings Technology 308 (2016) 168–173

[47] R. Y. Chau, W-S Ho, J.C. Wolfe, D. L. Licon, Effect of target temperature on the reactive d.c.-sputtering of silicon and niobium oxides, Thin Solid Films 287 (1996) 57-64

[48] K. K. Ho, K.P. Mohanchandra, G. P. Carman, examination of the sputtering profile of NiTi under target heating conditions, Thin Solid Films 413 (2002) 1–7

[49] T. P. Drüsedau, T. Bock, T.-M. John, F. Klabunde, and W. Eckstein, Energy transfer into the growing film during sputter deposition: An investigation by calorimetric measurements and Monte Carlo simulations, J. Vac. Sci. Technol. A Vacuum, Surfaces, Film., vol. 17, no. 5, (1999) 2896.

[50] S. Gauter, F. Haase, and H. Kersten, Experimentally unraveling the energy flux originating from a DC magnetron sputtering source, Thin Solid Films **669** (2018) 8-18.

[51] S. D. Ekpe and S. K. Dew, Theoretical and experimental determination of the energy flux during magnetron sputter deposition onto an unbiased substrate, J. Vac. Sci. Technol. A Vacuum, Surfaces, Film. **21** no. 2 (2003) 476.

[52] P. Kelly and R. Arnell, Magnetron sputtering: a review of recent developments and applications, Vacuum **56** (2000) 159

[53] N. Britun, T. Minea, S. Konstantinidis, and R. Snyders, Plasma diagnostics for understanding the plasma-surface interaction in HiPIMS discharges: A review, J. Phys. D. Appl. Phys. **47** (2014) 224001

[54] G. West, P. Kelly, P. Barker, A. Mishra, and J. Bradley, Measuremeents of deposition rate and substrate heating in a HiPIMS discharge, Plasma Processes Polym. 6(S1), (2009) S543–S547

[55] W.P. Leroy, S. Konstantinidis, S. Mahieu, R. Snyders, and D. Depla, Angular-resolved energy flux measurements of a dc- and HIPIMS-powered rotating cylindrical magnetron in reactive and non-reactive atmosphere, J. Phys. D. Appl. Phys. **44** (2011) 115201

[56] S. Berg, T. Nyberg, Fundamental understanding and modeling of reactive sputtering processes, Thin Solid Films 476 (2005) 215 – 230

[57] J. Musil, P. Baroch, J. Vlcˇek, K.H. Nam, J.G. Han, Reactive magnetron sputtering of thin films: present status and trends, Thin Solid Films 475 (2005) 208 – 218

[58] A.L. Thomann, P.A. Cormier, V. Dolique, N. Semmar, R. Dussart, T. Lecas, B. Courtois, P. Brault, Energy transferred to the substrate surface during reactive magnetron sputtering of aluminum in Ar/O2 atmosphere, Thin Solid Films 539 (2013) 88–95

[59] Jon M. Andersson, E. Wallin, E. P. Münger, and U. Helmersson, Energy distributions of positive and negative ions during magnetron sputtering of an Al target in Ar/O2 mixtures, J. Appl. Phys. 100 (2006) 033305

[60] S. Mráz and J.M. Schneider, Energy distribution of O-ions during reactive magnetron sputtering, Appl. Phys. Lett. **89** (2006) 51502

[51] S. Mráz and J.M. Schneider, Influence of the negative oxygen ions on the structure evolution of transition metal oxide thin films, J. Appl. Phys. 100 (2006) 23503

[62] K. Sarakinos, J. Alami, and S. Konstantinidis, High power pulsed magnetron sputtering: A review on scientific and engineering state of the art, Surf. Coatings Technol. 204 (2010) 1661–1684

[63] M. Bowes, P. Poolcharuansin, and J.W. Bradley, Negative ion energy distributions in reactive HiPIMS, J. Phys. D. Appl. Phys. **46 (**2013) 45204

[64] J. Bohlmark, M. Östbye, M. Lattemann, H. Ljungcrantz, T. Rosell, and U. Helmersson, Guiding the deposition flux in an ionized magnetron discharge, Thin Solid Films **515** (2006) 1928

[65] J. Alami, V. Stranak, A.-P. Herrendorf, Z. Hubicka, and R. Hippler, Plasma Sources Sci. Technol. Design of magnetic field configuration for controlled discharge properties in highly ionized plasma, **24**, (2015) 45016

[66] F Moens, T Kalvas, S Van Steenberge and D Depla, Effect of space charge on the negative oxygen flux during reactive sputtering, J. Phys. D: Appl. Phys. 50 (2017) 115201

[67] M. Raza, D. Cornil, J. Cornil, S. Lucas, R. Snyders, and S. Konstantinidis, Oxygen vacancy stabilized zirconia (OVSZ); a joint experimental and theoretical study, Scr. Mater. **124**, 26 (2016).

[68] M. Weise, S. Seeger, K. Harbauer, T. Welzel, K. & Ellmer, A multifunctional plasma and deposition sensor for the characterization of plasma sources for film deposition and etching, Journal of Applied Physics, 122 (2017) 044503

[69] K. Harbauer, T. Welzel, and K. Ellmer, A combined sensor for the diagnostics of plasma and film properties in magnetron sputtering processes, Thin Solid Films 520 (2012) 6429